BRITISH JOURNAL OF HOSPITAL MEDICINE

ARTICLE

Discrimination Model Construction for Non-Lactational Mastitis and Breast Cancer Based on Imaging Features

Jinjuan Peng[1,2], Meng Zhao[3], Shui Wang[1,*]

[1]Department of Breast Surgery, The First Affiliated Hospital with Nanjing Medical University, Nanjing, Jiangsu, China
[2]Department of Breast Surgery, The Fourth People's Hospital of Zhenjiang, Zhenjiang, Jiangsu, China
[3]Department of Radiology, The First Affiliated Hospital with Nanjing Medical University, Nanjing, Jiangsu, China
*Correspondence: shwang@njmu.edu.cn (Shui Wang)

Abstract

Aims/Background The clinical presentation of non-lactational mastitis (NLM) shares similarities with some symptoms and examination results of breast cancer (BC), which can lead to misdiagnosis or delayed treatment. Current studies on breast lesions mostly focus on the diagnostic performance of a single imaging technique. This study aims to construct a discrimination diagnostic model for NLM and BC based on such imaging features as ultrasound and magnetic resonance imaging (MRI) and to validate the application value of the model, assisting clinicians in improving disease diagnosis and refining medical decisions.

Methods This study is a retrospective analysis. Clinical data of 108 patients suspected of NLM based on imaging diagnosis, admitted to The First Affiliated Hospital with Nanjing Medical University between May 2018 and August 2023, were collected. Among them, 94 cases were pathologically confirmed as NLM and 14 cases as BC. Univariate and multivariate logistic regression analyses were performed on the patients' clinical data, ultrasound features, and MRI features to select the risk factors for discriminating NLM and BC, and construct a discrimination model. The discrimination performance of the model was analyzed with the receiver operating characteristic (ROC) curve, decision curve analysis (DCA), and calibration curve.

Results In the NLM group, there were 24 cases of granulomatous lobular mastitis (25.53%) and 70 cases of plasma cell mastitis (74.47%). In the BC group, there were 2 cases of infiltrating ductal carcinoma, 2 cases of atypical hyperplasia, 3 cases of papillary carcinoma, and 7 cases of ductal carcinoma *in situ*. Age, internal blood flow, calcification, edge, enhancement characteristics, apparent diffusion coefficient (ADC) values, and time-intensity curve (TIC) type were independent factors for differentiating NLM and BC ($p < 0.05$). The ROC analysis showed that the area under the curve of the model for discriminating NLM and BC was 0.920. The DCA results showed that the model had high net benefits for discriminating NLM and BC. The calibration curve analysis showed that the model had good consistency with the actual diagnosis of NLM and BC, with a chi-square value of 4.545 and a *p*-value of 0.155 according to the Hosmer–Lemeshow test.

Conclusion Age, internal blood flow, calcification, edge, enhancement characteristics, ADC, and TIC curve types are important factors in distinguishing NLM and BC, and the model based on the above characteristics to distinguish NLM and BC has a high net benefit in distinguishing the two.

Key words: non-lactational mastitis; breast cancer; imaging features; discrimination model

Submitted: 21 May 2024 Revised: 24 July 2024 Accepted: 1 August 2024

How to cite this article:
Peng J, Zhao M, Wang S. Discrimination Model Construction for Non-Lactational Mastitis and Breast Cancer Based on Imaging Features. Br J Hosp Med. 2024. https://doi.org/10.12968/hmed.2024.0278

Introduction

Non-lactational mastitis (NLM) refers to inflammation of the breast that occurs in women during non-lactating periods. The incidence of this disease is low (Jiao

et al, 2023). The pathogenesis of NLM is still not fully understood, but common causes include autoimmune factors, bacterial infections, milk stasis, and abnormal breast tissue (Shi et al, 2022). Clinical manifestations of NLM mainly include a painful breast lump with or without breast skin redness, nipple retraction, nipple discharge, and the presence of acute or chronic inflammation. It can progress to form multiple abscesses, persistent fistulas, and sinuses, leading to irreversible damage to the breast shape and significantly impacting the physical and mental health of affected patients. Despite being a benign condition, NLM exhibits "malignant" clinical behaviour, often characterized by recurrent episodes, prolonged disease course, and the potential to form fistulas and sinuses (Snider, 2022). In some cases, patients may opt for breast removal due to the persistent and distressing nature of the condition. Therefore, despite being a benign disease, NLM profoundly affects patients' well-being and quality of life. In the acute phase, symptoms may include redness, swelling, heat, pain, and the formation of abscesses or skin ulceration, for which antibiotic treatment is commonly recommended.

Breast cancer (BC) is a common malignant tumour in women, with an increasing incidence in recent years (Michaels et al, 2023). It poses a significant threat to women's lives, and current clinical treatment methods primarily include surgery, radiotherapy, and chemotherapy (Kunkler et al, 2023). Due to the different clinical presentations of NLM compared to benign conditions like fibroadenomas, as well as the similarity of some symptoms and examination results between NLM and BC, misdiagnosis or delayed treatment can occur. Therefore, accurate discrimination between NLM and BC is of utmost importance in developing personalized and precise treatment plans. Currently, pathological biopsy of breast tissue is considered the "gold standard" for distinguishing NLM from BC. However, this procedure is invasive and may lead to underestimation or overestimation of the lesion nature due to sampling bias, resulting in decreased accuracy (Martin et al, 2022).

With the continuous development of imaging techniques, ultrasound and magnetic resonance imaging (MRI) have been increasingly used in the differentiation and diagnosis of NLM and BC (Nakashima et al, 2019; Zhou et al, 2020). However, traditional imaging analysis is highly influenced by the subjective experience of physicians, resulting in limited diagnostic efficiency and potentially leading to unnecessary biopsies or inadequate clinical treatment (Dakhil et al, 2022). Currently, most studies on breast lesions focus on the diagnostic performance of a single imaging technique (Yu et al, 2022). The aim of this study is to construct a discrimination diagnostic model for NLM and BC based on ultrasound, MRI, and other imaging features, and to validate its clinical application value.

Methods

Research Objects

In this retrospective study, clinical data of 108 patients who were admitted to The First Affiliated Hospital with Nanjing Medical University and suspected of having NLM based on imaging diagnosis between May 2018 and August 2023 were collected. Among them, 94 cases were pathologically confirmed as NLM

and 14 cases as BC. The inclusion criteria were as follows: (1) age >18 years; (2) suspected NLM based on imaging diagnosis, complete ultrasound, MRI, and other imaging data; and (3) complete clinical information. The exclusion criteria were as follows: (1) incomplete or poor-quality imaging data; (2) history of biopsy, surgery, radiotherapy, chemotherapy, or medication before imaging examination; (3) unclear nature of the lesion; and (4) pathological diagnosis; and pregnant or lactating women. This study complied with the "Helsinki Declaration" and was approved by the Medical Ethics Committee of The First Affiliated Hospital with Nanjing Medical University (2024-SR-134). All patients in this study signed informed consent.

Ultrasound Examination

Ultrasound examinations were performed with the ultrasound diagnostic instruments MyLab Twice LA523 (Esaote, Genova, Italy) and AixPlorer SL15-4 (SuperSonic Imagine, Provence, France) with a probe frequency of 4–13 MHz. The examination methods were as follows: the patient was placed in a supine or contralateral oblique position, adequately exposing the breast and axilla. The display of the deep pectoralis major muscle and ribs was used as an adjustment standard. The transducer was positioned perpendicular to the chest wall, and both radial and longitudinal scan modes were used. Initially, a routine two-dimensional ultrasound examination of the breast was performed, followed by a multi-planar scan of the regions of interest or areas with lesions. The nodular characteristics and axillary lymph nodes were carefully observed in different planes. The largest cross-section of the mass was analyzed, and the blood flow inside and around the lesion was examined. Ultrasound features, including shape (regular/irregular), internal blood flow (scanty or absent/rich), calcification (present/absent), edge (smooth/irregular), internal echo pattern (homogeneous/heterogeneous), and ultrasound Breast Imaging Reporting and Data System (BI-RADS) classification, were recorded. All imaging data were evaluated by two ultrasound diagnostic physicians with a blinded method. In cases where there was disagreement between the two physicians, a consensus was reached through discussion.

MRI Examination

MRI examinations were performed using the uMR OMEGA 3.0T MRI (United Imaging, Shanghai, China) scanner with a 24-channel breast phased-array coil. The scanning sequences included non-contrast sequences and contrast-enhanced sequences. The non-contrast sequences consisted of T1-weighted imaging (T1WI), T2WI fat-suppressed imaging (STIR), and diffusion-weighted imaging (DWI). The contrast-enhanced sequences included dynamic contrast-enhanced T1WI, T2WI fat-suppressed imaging (sag), and T1WI (cor). The parameters for the non-contrast sequences were as follows: repetition time (TR) for T1WI was 547 ms, echo time (TE) was 7.52 ms, and field of view (FOV) was 300 mm × 340 mm; TR for T2WI (stir) was 5948 ms, TE was 79.86 ms, and FOV was 300 mm × 340 mm; TR for DWI was 6952 ms, TE was 72.6 ms, and FOV was 350 mm × 190 mm. The slice thickness for all three sequences was 3.5 mm with a 0.9 mm interslice gap. The

parameters for the contrast-enhanced sequences were as follows: TR for dynamic T1WI was 5 ms, TE was 1.96 ms, FOV was 300 mm × 340 mm, and the slice thickness was 1.3 mm with a 0.3 mm interslice gap; TR for T2WI fat-suppressed (sag) was 2856 ms, TE was 63.72 ms, FOV was 230 mm × 230 mm, and the slice thickness was 3.5 mm with a 0.3 mm interslice gap; TR for T1WI (cor) was 3.99 ms, TE was 1.3/2.24 ms, FOV was 380 mm × 380 mm, and the slice thickness was 3 mm with a 0.3 mm interslice gap.

Examination method: The patient was positioned in a prone position, with the breasts naturally hanging inside the coil. The scanning range included both breasts, the corresponding anterior chest wall, and the axilla. A total of six cycles of dynamic contrast-enhanced scanning were performed. The first cycle was a pre-scan using the fat-suppressed T1WI imaging sequence. Then, a contrast agent was injected through the elbow vein using a high-pressure injector (the contrast agent used was Gd-DTPA Magnevist (KTOLOB3, Bayer, Leverkusen, Germany) with a formulation of 15 mL/7.035 g and a dose of 0.2 mmol/kg, at a flow rate of 3.0 mL/s). Following the contrast injection, a saline flush of 15 mL was administered, completing the entire injection within 20 seconds. After the contrast injection, five consecutive scan cycles were performed, with each cycle lasting approximately 60 seconds.

Image processing method: All original images of the cases were uploaded to the image processing workstation. The scan sequence images were observed, and the MRI features were described according to the 5th edition of the BI-RADS standard developed by the American College of Radiology in 2013 (Shin et al, 2017). The region of interest delineation selected the solid area on the plane where the maximum diameter of the lesion is located for measurement, avoiding cystic changes, necrosis, and calcification within the lesion, and avoiding visible vessels around the lesion. The apparent diffusion coefficient (ADC) value was measured twice, and the average value was taken. At the same time, the time-intensity curve (TIC) of the lesion was obtained. All imaging data were evaluated by two MR diagnostic physicians with a blinded method. When the opinions of the two individuals were inconsistent, a consensus was reached through discussion.

Discriminant Diagnosis Model Construction

The 108 cases of NLM and BC patients who underwent ultrasound and MRI examinations were divided into the NLM group (n = 94) and the BC group (n = 14). Stepwise logistic regression analysis was used to further select features, and the optimal feature subset with a significant level of $p < 0.05$ was retained. A radiation feature model based on logistic regression was established and visualized using forest maps. The discriminative ability of the predictive model was evaluated with the area under the curve (AUC), where a larger AUC indicates better discriminative ability of the predictive model. The model performance was evaluated based on AUC, sensitivity, specificity, and accuracy. The calibration of the model was evaluated by the calibration curve and the Hosmer–Lemeshow chi-square test. The calibration curve reflects the consistency between the risk of identifying BC and

NLM and the real risk in patients with different risk stratification. Decision curve analysis (DCA) was used to evaluate the clinical practicability of the model.

Statistical Analysis

The collected data were analyzed with SPSS 27.0 (IBM, New York, NY, USA) and R software (version 4.3.1, University of Auckland, Auckland, New Zealand). All data were tested for normality using the Shapiro–Wilk test. Normally distributed continuous variables were presented as the mean ± standard deviation ($\bar{x} \pm s$), and the independent samples *t*-test was used for comparison between groups. Categorical data were expressed as frequency or rate and associations were assessed using the chi-square test, continuity-corrected chi-square test, or Fisher's exact test. A significance level of $p < 0.05$ was considered statistically significant for all analyses.

Results

Comparison of General Information between the NLM Group and the BC Group

The NLM group consisted of patients aged 23 to 71 years, with a mean age of 37.43 ± 9.25 years and an average duration of illness of (6.25 ± 1.28) months. The tumour locations were as follows: 53 cases in the left breast and 41 cases in the right breast. Among them, 24 cases (25.53%) were diagnosed with granulomatous lobular mastitis, and 70 cases (74.47%) were diagnosed with plasma cell mastitis. The BC group consisted of patients aged 27 to 58 years, with a mean age of 44.71 ± 8.23 years and an average duration of illness of 5.92 ± 1.95 months. The tumour locations were as follows: 9 cases in the left breast and 5 cases in the right breast. The diagnoses in the BC group included 2 cases of invasive ductal carcinoma, 2 cases of atypical hyperplasia, 3 cases of papillary carcinoma, and 7 cases of ductal carcinoma *in situ*. There was a significant difference in age between the NLM and BC groups ($p = 0.007$). There were no significant differences in the course of the disease, location of the tumour, or other baseline data ($p > 0.05$) (Table 1).

Comparison of Ultrasound Features between the NLM Group and the BC Group

There were significant differences in internal blood flow ($p = 0.040$), shape of mass edge ($p = 0.019$), and calcification ($p < 0.001$) between the NLM group and the BC Group ($p < 0.05$). There were no significant differences in other ultrasonic features between the two groups ($p > 0.05$) (Table 2).

Comparison of MRI Features between the NLM Group and the BC Group

There were significant differences between the NLM Group and the BC Group in enhancement characteristics ($p = 0.010$), ADC value ($p < 0.001$), and TIC curve types ($p = 0.003$). There were no significant differences in other features between the two groups ($p > 0.05$, Table 3).

Table 1. Comparison of baseline data between the NLM group and the BC group.

Data	NLM group (n = 94)	BC group (n = 14)	χ^2/t	*p*-value
Age (cases)			7.166	0.007
<60 years	62	4		
≥60 years	32	10		
Course of disease (months, $\bar{x} \pm s$)	6.25 ± 1.28	5.92 ± 1.95	0.835	0.406
Location of mass (cases)			0.311	0.577
Left breast	53	9		
Right breast	41	5		
Basic medical history (cases)			0.008	0.931
Yes	22	4		
No	72	10		
First-degree family history (cases)			0.257	0.613
Yes	6	2		
No	88	12		

NLM, non-lactational mastitis; BC, breast cancer.

Risk Factors for Differentiating NLM from BC with Logistic Regression

Multivariate logistic regression analysis was performed on the variables with statistically significant differences in Tables 1,2,3. Taking BC and NLM as dependent variables (NLM = 0, BC = 1), the assignment of independent variables is shown in Table 4. Multivariate logistic regression analysis showed that age ($p < 0.001$), internal blood flow ($p < 0.05$), calcification ($p < 0.05$), shape of mass edge ($p < 0.05$), enhancement characteristics ($p < 0.05$), lesion ADC value ($p < 0.001$), and TIC curve type ($p < 0.001$) were independent risk factors for differentiating NLM from BC (Table 5).

Differentiation Model Construction and Evaluation

Based on the statistically significant factors identified in the logistic regression analysis, a predictive model for differentiation was established. The forest map was drawn according to the results of the multivariate logistic regression multivariate analysis. It can be seen that age, internal blood flow, TIC curve, calcification, ADC, and enhancement characteristics were all positive risk factors, which did not intersect with the invalid line (as shown in Fig. 1). The receiver operating characteristic (ROC) analysis results revealed that the AUC of the model for differentiating NLM and BC was 0.920 (as shown in Fig. 2). On the basis of the identification model, the screened risk factors were subjected to DCA for NLM and BC identification. The results showed that when the risk threshold of the model to identify NLM and BC was >0.03, it provided a significant increase in clinical net benefit; when the risk threshold was >0.25, the clinical net benefit of the prediction model was significantly higher than that of a single predictor (as shown in Fig. 3). The calibration curve analysis results show good consistency between the model's differentiation of NLM and BC and the actual diagnosis, with a Hosmer–Lemeshow chi-square statistic of 4.545 and a *p*-value of 0.155 (as shown in Fig. 4).

Table 2. Comparison of ultrasound features between the NLM group and the BC group.

Feature	NLM group (n = 94)	BC group (n = 14)	χ^2 value	*p*-value
Shape (cases)			-	0.575
Symmetrical	5	1		
Asymmetrical	89	13		
Internal blood flow (cases)			-	0.040
Minimal or absent	43	2		
Abundant	51	12		
Calcifications (cases)			17.491	<0.001
Present	12	9		
Absent	82	5		
Shape of mass edge (cases)			-	0.019
Smooth	28	0		
Irregular	66	14		
Internal echoes (cases)			0.027	0.871
Homogeneous	12	1		
Heterogeneous	82	13		
Ultrasound BI-RADS classification			-	0.663
Category 3	40	8		
Category 4a	46	5		
Category 4b	7	1		
Category 4c	1	0		

NLM, non-lactational mastitis; BC, breast cancer; BI-RADS, breast imaging reporting and data system.

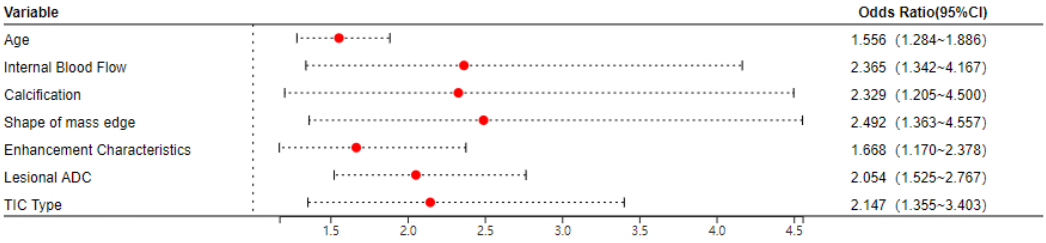

Fig. 1. Forest plot of risk factors for differentiation of NLM and BC. NLM, non-lactational mastitis; BC, breast cancer; ADC, apparent diffusion coefficient; TIC, time-intensity curve.

Discussion

The specific pathogenesis of NLM is currently not clear. It is often associated with developmental abnormalities, involution, and dilation of the milk ducts caused by degeneration and shedding of the epithelial cells lining the ducts (Zhou et al, 2022). The inflammatory response mainly manifests as necrotic lesions in the surrounding adipose tissue of the breast, and the inflammation can also affect the lobules of the breast. In patients with BC, there is malignant tissue in the surrounding breast tissue, and irregular proliferation of the ductal epithelium, disrupted secretion function, and accumulation of lipid-like secretions in the large ducts beneath the nipple or areola can be observed. Therefore, the clinical symptoms of

Table 3. Comparison of magnetic resonance imaging (MRI) features between the NLM group and the BC group.

Feature	NLM group (n = 94)	BC group (n = 14)	χ^2/t value	*p*-value
Distribution (cases)			3.531	0.317
Regional	19	1		
Segmental	25	4		
Diffuse	34	4		
Other	16	5		
Enhancement characteristics (cases)			9.181	0.010
Heterogeneous	49	2		
Clustering	11	1		
Rim enhancement	34	11		
ADC ($\times 10^{-3}$ mm^2/s, $\bar{x} \pm s$)	1.12 ± 0.18	0.74 ± 0.29	6.739	<0.001
TIC type (cases)			11.612	0.003
Wash-in	16	8		
Plateau	41	4		
Wash-out	37	2		

NLM, non-lactational mastitis; BC, breast cancer; ADC, apparent diffusion coefficient; TIC, time-intensity curve.

Table 4. Variable assignment.

Variable	Assigning methods
Age	<60 years = 0, ≥60 years = 1
Internal blood flow	Minimal or absent = 0, Abundant = 1
Calcification	Absent = 0, Present = 1
Shape of mass edge	Smooth = 0, Irregular = 1
Enhancement characteristics	Heterogeneous/Clustering = 0, Rim enhancement = 1
ADC	Primitive value
TIC type	Wash-out/Plateau = 0, = 2, Wash-in = 1

BC and NLM are similar (Sun et al, 2024; Tang et al, 2024), which increases the difficulty in distinguishing these two conditions.

Based on ultrasound observation of the lesion images and characteristics of NLM and BC, there are no differences in terms of lesion shape, edge, and internal echogenicity. However, there is a statistically significant difference in the presence of calcifications, which can be considered an important ultrasound feature for distinguishing between the two conditions (Wang et al, 2023). Large calcifications are typically associated with such benign conditions as breast cysts, calcified fibroadenomas, or senile calcifications. They usually appear as larger patchy or nodular calcifications and are generally not associated with breast cancer. Microcalcifications, on the other hand, may indicate potential malignant lesions. They appear as small and subtle calcifications that can be clearly seen under magnification. When microcalcifications cluster together, it may indicate an increased likelihood of BC (Hester et al, 2021; Yigitbasi et al, 2017). In the present study, both groups showed

Table 5. Risk factors for differentiating NLM and BC with logistic regression.

Variable	β	SE	Wald χ^2	p-value	OR	95% CI
Age (≥60 years)	0.442	0.098	20.353	<0.001	1.556	1.284–1.886
Internal blood flow (Abundant)	0.861	0.289	8.871	<0.05	2.365	1.342–4.167
Calcification (Present)	0.845	0.336	6.331	<0.05	2.329	1.205–4.500
Shape of mass edge (Irregular)	0.913	0.308	8.789	<0.05	2.492	1.363–4.557
Enhancement characteristics (Rim enhancement)	0.512	0.181	7.990	<0.05	1.668	1.170–2.378
ADC	0.720	0.152	22.425	<0.001	2.054	1.525–2.767
TIC type (Wash-in)	0.764	0.235	10.571	<0.001	2.147	1.355–3.403

ADC, apparent diffusion coefficient; TIC, time-intensity curve; OR, odds ratio; CI, confidence interval.

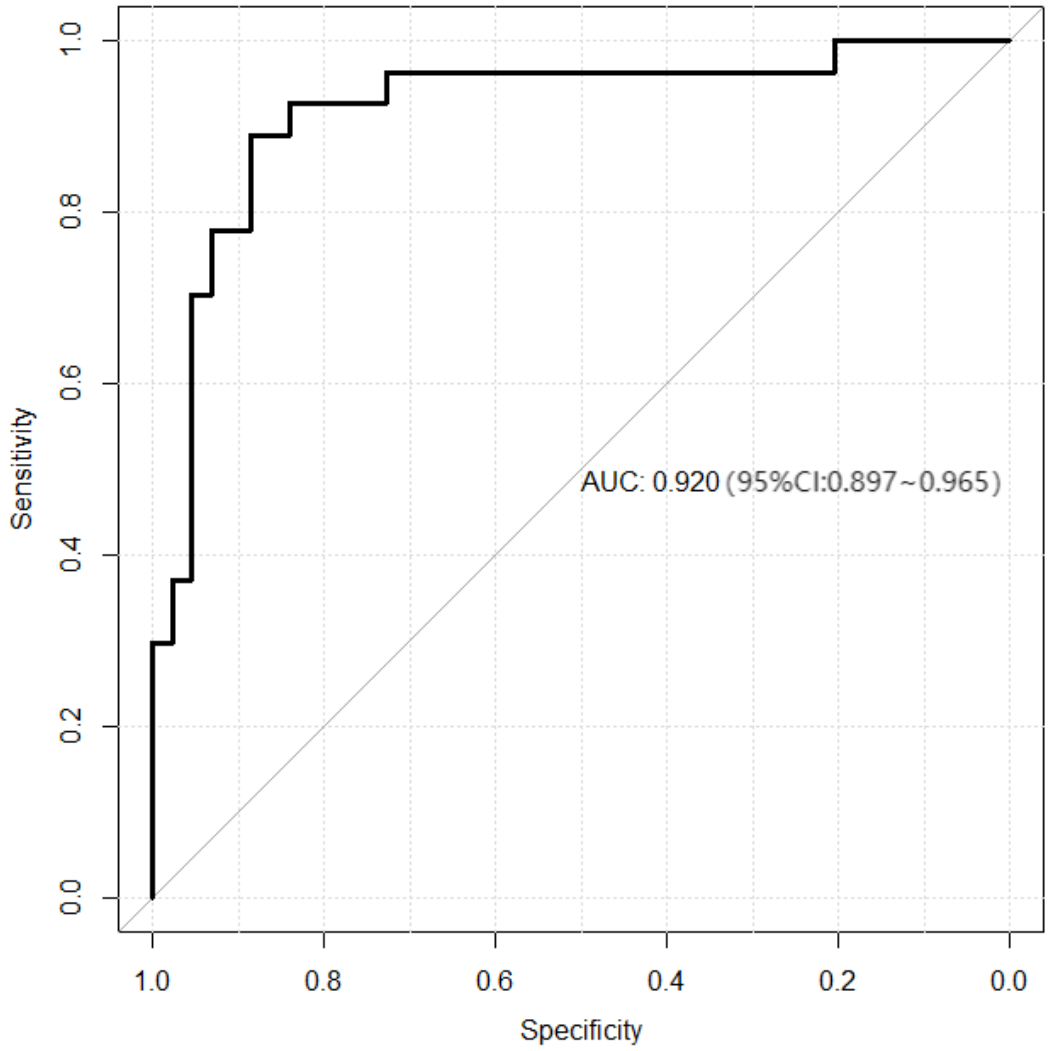

Fig. 2. Receiver operating characteristic (ROC) curve for differentiating NLM and BC.

a high proportion of rich internal blood flow signals. The reason for this could be related to the pathogenesis of granulomatous lobular mastitis and the local granulomatous reaction. Granulomatous changes can lead to inflammatory reactions in the surrounding tissues, causing local symptoms such as pain and swelling. The

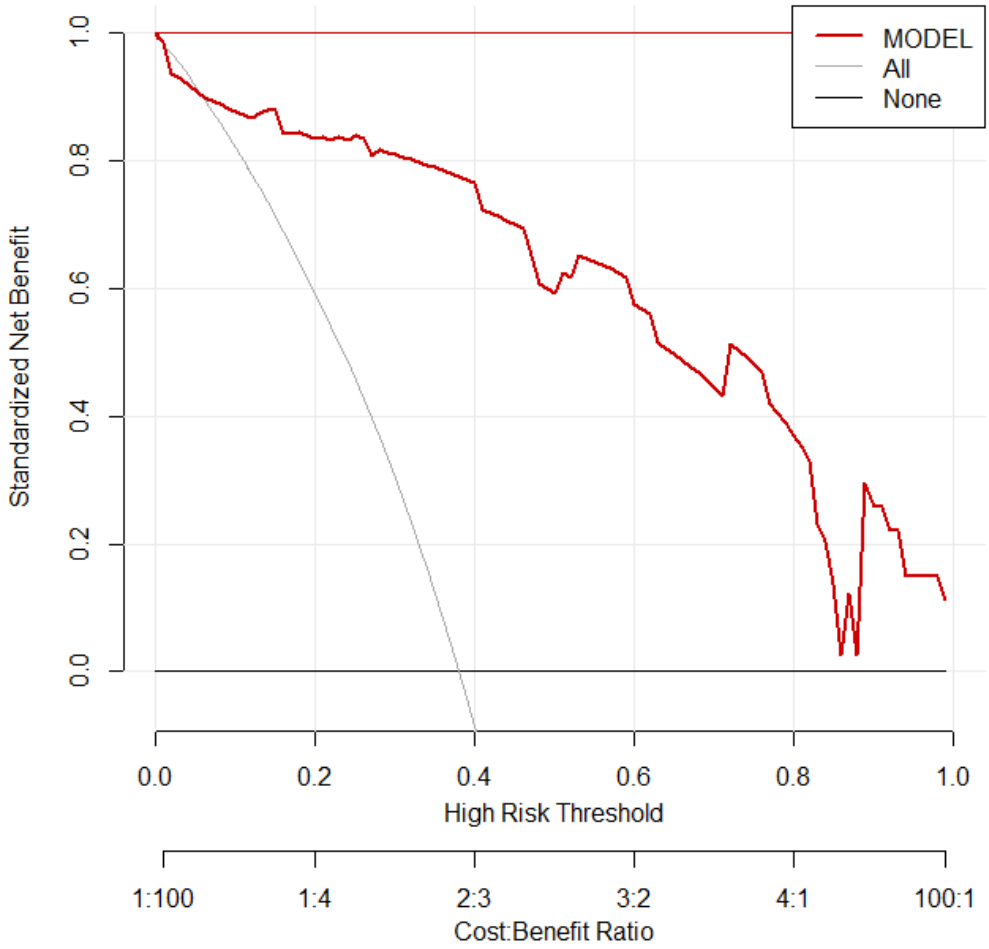

Fig. 3. Decision curve analysis (DCA) for NLM and BC differentiation.

process of fat necrosis, abscess formation, and fibrosis within the lesion can further disrupt the normal anatomical structure of the breast and may have an impact on breast function and morphology (Velidedeoglu et al, 2021).

A comparison of the lesion images and characteristics of NLM and BC through MRI reveals that there are no differences in terms of distribution, enhancement characteristics, and lesion ADC values. However, there is a statistically significant difference in the type of TIC, which indicates that the value of using MRI alone to differentiate between the two conditions is also limited. DWI enables non-invasive observation of the movement of water molecules within the body. The ADC value indirectly reflects this movement of water molecules in breast lesions, aiding in the differential diagnosis of benign and malignant breast lesions. Due to the rapid proliferation of cancer cells in breast cancer, high cell density, decreased extracellular volume, larger nuclei, and reduced cytoplasm, the movement of water molecules within the cells slows down. This results in higher DWI signal intensity than that of surrounding normal tissue and lower ADC values (Chen et al, 2020; Zhao et al, 2020). In the present study, there was no statistical difference in ADC values

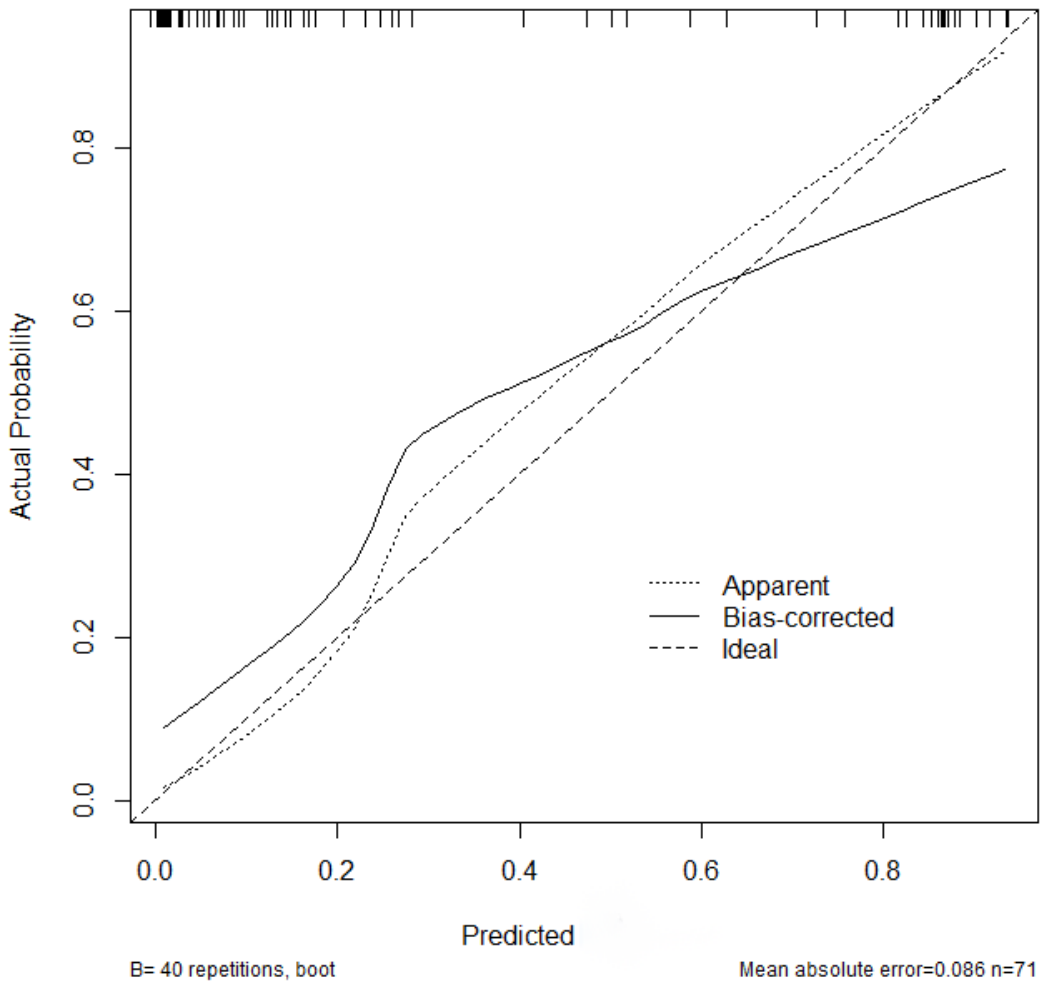

Fig. 4. Calibration curve for NLM and BC differentiation.

between the two groups, which may be due to the small sample size of the BC group. Dynamic contrast-enhanced MRI not only allows the observation of signal characteristics and lesion morphology but also provides information on the TIC and enhancement features of the lesions, indirectly reflecting tumour angiogenesis (Yin, 2019). To some extent, TIC can reflect the vascular microenvironment of the lesion. In some BC lesions, due to the incomplete development and weak walls of tumour neovasculature, contrast agents may rapidly wash out, resulting in an "outflow" type of TIC. Additionally, non-mass-like BC lesions have normal glandular tissue within them, and tumour cells can obtain nutrients from the blood vessels within the normal glands, which can also affect the morphology of the TIC (Chung et al, 2023; Qu et al, 2020). Therefore, the TIC of these lesions often exhibits dynamic characteristics. In contrast, the blood vessels within breast inflammatory lesions usually do not have the characteristics of tumour neovasculature. The increased blood flow, increased permeability, and vascular dilation in the inflammatory area mostly result in progressive or plateau-type TIC (Wekking et al, 2023). This type of TIC differs from the dynamic TIC of BC, so combining clinical presentation and other imaging features can help differentiate between inflammation and cancer.

A study has pointed out that the breast BI-RADS classification based on morphological features is indeed influenced to some extent by the subjective experience and accumulation of ultrasound physicians (Lobbes et al, 2021). The lack of quantitative indicators may reduce the consistency and reliability of the diagnosis. However, with the development of artificial intelligence and big data technology, predictive models have emerged, providing new ideas and tools for the diagnosis and assessment of BC. Building models can extract deep-level imaging features from breast tumour images and use machine learning techniques to analyze and model these data. By learning from a large amount of imaging data, the model can discover patterns hidden in the data and use them for risk prediction of breast diseases and assistance in clinical decision-making (Kayadibi et al, 2022).

This study conducted single-factor and multi-factor logistic regression to screen for risk factors in differentiating NLM and BC. After the selection, age, internal blood flow, calcifications, edges, enhancement characteristics, lesion ADC, and TIC curve type were identified as independent factors in distinguishing between NLM and BC. Based on these factors, a discriminative model was constructed, and its discriminative value was analyzed with ROC curves, DCA, and calibration curves. The ROC analysis results showed that the AUC of the model in differentiating NLM and BC was 0.920. The DCA results indicated that the model had a high net benefit in distinguishing NLM and BC. The calibration curve analysis results demonstrated good consistency between the model's predictions and the actual diagnosis of NLM and BC. This study has certain limitations, like the single-centre retrospection and the inclusion of relatively limited parameters. Future research should consider incorporating qualitative and quantitative indicators from contrast-enhanced ultrasound, and increasing the sample size, in order to further validate the research findings.

Conclusion

In conclusion, the model constructed based on imaging features for distinguishing between NLM and BC has a high discriminative value, effectively addressing the challenge faced by primary care and less-experienced doctors in quantitatively evaluating the similarities between the two groups of symptoms. These results can inform treatment strategies and assist in clinical decision-making.

Key Points

- Age, internal blood flow, calcification, edge, enhancement characteristics, lesion ADC, and TIC curve types were independent risk factors for identifying breast cancer (BC) and non-lactating mastitis (NLM).
- By screening the risk factors for identifying NLM and BC and constructing a differential model, it was found that the area under the curve of the model for identifying BC and NLM was 0.920.
- The model has a higher net benefit in identifying NLM and BC.
- The model has good consistency with the actual diagnosis in identifying NLM and BC.

Availability of Data and Materials

All data included in this study are available upon request by contact with the corresponding author.

Author Contributions

JJP and SW designed the research. JJP and MZ performed the research and analyzed the data. JJP drafted the manuscript. All authors contributed to the important editorial changes in the manuscript. All authors read and approved the final manuscript. All authors have participated sufficiently in the work and agreed to be accountable for all aspects of the work.

Ethics Approval and Consent to Participate

This study was approved by the Medical Ethics Committee of The First Affiliated Hospital with Nanjing Medical University (2024-SR-134). All patients in this study signed informed consent.

Acknowledgement

Not applicable.

Funding

This research received no external funding.

Conflict of Interest

The authors declare no conflict of interest.

References

Chen R, Hu B, Zhang Y, Liu C, Zhao L, Jiang Y, et al. Differential diagnosis of plasma cell mastitis and invasive ductal carcinoma using multiparametric MRI. Gland Surgery. 2020; 9: 278–290. https://doi.org/10.21037/gs.2020.03.30

Chung M, Calabrese E, Mongan J, Ray KM, Hayward JH, Kelil T, et al. Deep Learning to Simulate Contrast-enhanced Breast MRI of Invasive Breast Cancer. Radiology. 2023; 306: e213199. https://doi.org/10.1148/radiol.213199

Dakhil HA, Easa AM, Hussein AY, Bustan RA, Najm HS. Diagnostic role of dynamic contrast-enhanced magnetic resonance imaging in differentiating breast lesions. Journal of Population Therapeutics and Clinical Pharmacology. 2022; 29: e88–e94. https://doi.org/10.47750/jptcp.2022.912

Hester RH, Hortobagyi GN, Lim B. Inflammatory breast cancer: early recognition and diagnosis is critical. American Journal of Obstetrics and Gynecology. 2021; 225: 392–396. https://doi.org/10.1016/j.ajog.2021.04.217

Jiao Y, Chang K, Jiang Y, Zhang J. Identification of periductal mastitis and granulomatous lobular mastitis: a literature review. Annals of Translational Medicine. 2023; 11: 158. https://doi.org/10.21037/atm-22-6473

Kayadibi Y, Kocak B, Ucar N, Akan YN, Yildirim E, Bektas S. MRI Radiomics of Breast Cancer: Machine Learning-Based Prediction of Lymphovascular Invasion Status. Academic Radiology. 2022; 29: S126–S134. https://doi.org/10.1016/j.acra.2021.10.026

Kunkler IH, Williams LJ, Jack WJL, Cameron DA, Dixon JM. Breast-Conserving Surgery with or without Irradiation in Early Breast Cancer. New England Journal of Medicine. 2023; 388: 585–594. https://doi.org/10.1056/NEJMoa2207586

Lobbes MBI, Heuts EM, Moossdorff M, van Nijnatten TJA. Contrast enhanced mammography (CEM) versus magnetic resonance imaging (MRI) for staging of breast cancer: The pro CEM perspective. European Journal of Radiology. 2021; 142: 109883. https://doi.org/10.1016/j.ejrad.2021.109883

Martin EA, Chauhan N, Dhevan V, George E, Laskar P, Jaggi M, et al. Current status of biopsy markers for the breast in clinical settings. Expert Review of Medical Devices. 2022; 19: 965–975. https://doi.org/10.1080/17434440.2022.2159807

Michaels E, Worthington RO, Rusiecki J. Breast Cancer: Risk Assessment, Screening, and Primary Prevention. The Medical Clinics of North America. 2023; 107: 271–284. https://doi.org/10.1016/j.mcna.2022.10.007

Nakashima K, Uematsu T, Harada TL, Takahashi K, Nishimura S, Tadokoro Y, et al. MRI-detected breast lesions: clinical implications and evaluation based on MRI/ultrasonography fusion technology. Japanese Journal of Radiology. 2019; 37: 685–693. https://doi.org/10.1007/s11604-019-00866-8

Qu N, Luo Y, Yu T. Differentiation between Clinically Noninflammatory Granulomatous Lobular Mastitis and Noncalcified Ductal Carcinoma in situ Using Dynamic Contrast-Enhanced Magnetic Resonance Imaging. Breast Care. 2020; 15: 619–627. https://doi.org/10.1159/000506068

Shi L, Wu J, Hu Y, Zhang X, Li Z, Xi PW, et al. Biomedical Indicators of Patients with Non-Puerperal Mastitis: A Retrospective Study. Nutrients. 2022; 14: 4816. https://doi.org/10.3390/nu14224816

Shin K, Phalak K, Hamame A, Whitman GJ. Interpretation of Breast MRI Utilizing the BI-RADS Fifth Edition Lexicon: How Are We Doing and Where Are We Headed? Current Problems in Diagnostic Radiology. 2017; 46: 26–34. https://doi.org/10.1067/j.cpradiol.2015.12.001

Snider HC. Management of Mastitis, Abscess, and Fistula. The Surgical Clinics of North America. 2022; 102: 1103–1116. https://doi.org/10.1016/j.suc.2022.06.007

Sun J, Shao S, Wan H, Wu X, Feng J, Gao Q, et al. Prediction models for postoperative recurrence of non-lactating mastitis based on machine learning. BMC Medical Informatics and Decision Making. 2024; 24: 106. https://doi.org/10.1186/s12911-024-02499-y

Tang H, Wu X, Feng J, Gao Q, Shao S, Qu W, et al. Adolescent Non-Puerperal Mastitis: Risk Factors, Clinical Characteristics, and Prognosis Analysis. Journal of Inflammation Research. 2024; 17: 487–495. https://doi.org/10.2147/JIR.S447181

Velidedeoglu M, Kundaktepe BP, Aksan H, Uzun H. Preoperative Fibrinogen and Hematological Indexes in the Differential Diagnosis of Idiopathic Granulomatous Mastitis and Breast Cancer. Medicina. 2021; 57: 698. https://doi.org/10.3390/medicina57070698

Wang Z, Hua L, Liu X, Chen X, Xue G. A hematological parameter-based model for distinguishing non-puerperal mastitis from invasive ductal carcinoma. Frontiers in Oncology. 2023; 13: 1295656. https://doi.org/10.3389/fonc.2023.1295656

Wekking D, Porcu M, De Silva P, Saba L, Scartozzi M, Solinas C. Breast MRI: Clinical Indications, Recommendations, and Future Applications in Breast Cancer Diagnosis. Current Oncology Reports. 2023; 25: 257–267. https://doi.org/10.1007/s11912-023-01372-x

Yigitbasi MR, Guntas G, Atak T, Sonmez C, Yalman H, Uzun H. The Role of Interleukin-33 as an Inflammatory Marker in Differential Diagnosis of Idiopathic Granulomatous Mastitis and Breast Cancer. Journal of Investigative Surgery. 2017; 30: 272–276. https://doi.org/10.1080/08941939.2016.1240270

Yin Q. The diagnostic value of MRI multi-parameter combination for breast lesions with ring enhancement. Journal of B.U.ON. 2019; 24: 509–515.

Yu Y, Ye X, Yang J, Chen L, Zhang M, He Y, et al. Application of a shear-wave elastography prediction model to distinguish between benign and malignant breast lesions and the adjustment of ultrasound Breast Imaging Reporting and Data System classifications. Clinical Radiology. 2022; 77: e147–e153. https://doi.org/10.1016/j.crad.2021.10.016

Zhao Q, Xie T, Fu C, Chen L, Bai Q, Grimm R, et al. Differentiation between idiopathic granulomatous mastitis and invasive breast carcinoma, both presenting with non-mass enhancement without rim-enhanced masses: The value of whole-lesion histogram and texture analysis using apparent diffusion coefficient. European Journal of Radiology. 2020; 123: 108782. https://doi.org/10.1016/j.ejrad.2019.108782

Zhou J, Zhang Y, Chang KT, Lee KE, Wang O, Li J, et al. Diagnosis of Benign and Malignant Breast Lesions on DCE-MRI by Using Radiomics and Deep Learning With Consideration of Peritumor Tissue. Journal of Magnetic Resonance Imaging. 2020; 51: 798–809. https://doi.org/10.1002/jmri.26981

Zhou Y, Feng BJ, Yue WW, Liu Y, Xu ZF, Xing W, et al. Differentiating non-lactating mastitis and malignant breast tumors by deep-learning based AI automatic classification system: A preliminary study. Frontiers in Oncology. 2022; 12: 997306. https://doi.org/10.3389/fonc.2022.997306